DEVELOPMENT OF MACRO-MODEL SEISMIC COLLAPSE SIMULATOR FOR FRAMED STRUCTURES USING ASI-GAUSS TECHNIQUE

N. Katahira[1], D. Isobe[2], T. Ine[3] and K. Kajiwara[4]

[1] *Graduate Student, University of Tsukuba, Japan*
[2] *Associate Professor, Dept. of Engineering Mechanics and Energy, University of Tsukuba, Japan*
[3] *Invited Research Fellow, National Research Institute for Earth Science and Disaster Prevention, Japan*
[4] *Senior Researcher, National Research Institute for Earth Science and Disaster Prevention, Japan*
Email: e0311273@edu.esys.tsukuba.ac.jp, isobe@kz.tsukuba.ac.jp, ine@bosai.go.jp, kaji@bosai.go.jp

ABSTRACT :

The main objective of this study is to develop a macro-model finite element code, which can simulate dynamic behaviors with strong nonlinearities and discontinuities and is efficiently applicable to seismic collapse analyses of framed structures. The applied technique is called the ASI-Gauss technique for the linear Timoshenko beam element, which computes highly accurate elasto-plastic solutions even with the minimum number of elements per member. It gains high accuracy especially in elastic range, by placing the numerical integration points of the two consecutive elements forming an elastically deformed member in such a way that stresses and strains are evaluated at the Gaussian integration points of the two-element member. Moreover, the technique can be used to express member fracture, by shifting the numerical integration point to an appropriate position and by releasing the resultant forces in the element simultaneously. The numerical code can be used to analyze dynamic behaviors of framed structures, initiating from elastic range to a total collapse. Simple numerical tests are conducted in this paper to verify the proposed code. Moreover, a three-dimensional seismic collapse analysis considering member fracture and contact is performed on a large-scale framed structure, and practical results are obtained in a reasonable short calculation time.

KEYWORDS: Seismic collapse simulator, Framed structures, ASI-Gauss technique, Linear Timoshenko beam element, Non-linear FEM

1. INTRODUCTION

In the conventional design of a building, only static analysis in the horizontal and uniaxial directions is commonly carried out, in order to minimize calculation costs. This approach can ensure the structural strength of the building, if there is sufficient strength to support the load in the vertical direction. For a similar reason, the mass system model replaces the building layer in dynamic analysis, and the complicated dynamic behavior of the structure at the member level becomes difficult to be examined sufficiently. Therefore, the development of a more precise and more efficient dynamic analysis code is strongly desired.

Recently, significant advances in the field of computers have been eliminating the calculation cost restrictions, and various dynamic analysis codes are being developed. Among those codes, there are some codes applicable to dynamic collapse problems which contain strong nonlinearities and discontinuities, such as the Distinct Element Method (DEM) [1] or the Discontinuous Deformation Analysis (DDA) [2]. These codes have been applied to demolition analyses and seismic collapse analyses [3-6]. However, the above-mentioned discrete numerical methods are computationally intensive and need detailed modeling. Therefore, they are suitable only for detailed analyses of either two-dimensional or small three-dimensional models.

On the other hand, the Finite Element Method (FEM), which is based on continuum material equations, has been successfully applied to a wide range of engineering problems including structural analyses of large-scale structures. However, the FEM is generally limited to analyses of relatively small displacements and it needs complicated modifications to simulate fracture occurring in structural members or joints. The main objective of this study is to develop a finite element seismic collapse simulator, which can simulate dynamic behaviors with such strong nonlinearities and discontinuities and is efficiently applicable to seismic collapse problems of framed structures.

Toi and Isobe developed the Adaptively Shifted Integration (ASI) technique [7,8] for the linear Timoshenko beam and the Bernoulli-Euler beam elements, which can be easily implemented into the existing finite element codes. In this technique, the numerical integration point is shifted immediately after the occurrence of a fully plastic section in the element so that a plastic hinge is formed exactly at that section. As a result, the ASI technique gives more precise elasto-plastic solutions than the conventional schemes, and has become able to simulate dynamic behaviors with strong nonlinearities by using only a small number of elements for a member. Structurally discontinuous problems have also become easily handled, by shifting the numerical integration point of the linear Timoshenko beam element to an appropriate position, and by releasing the resultant forces in the element simultaneously [9,10]. However, when the number of elements per member is very small, it still lacks accuracy in the elastic range compared to the converged solution, due to the low-order displacement function of the linear Timoshenko beam element.

To improve the accuracy in elastic range, Isobe and Lynn modified the ASI technique into an ASI-Gauss technique [11]. The accuracy in elastic range is improved by placing the numerical integration points of the two consecutive elements forming an elastically deformed member in such a way that stresses and strains are evaluated at the Gaussian integration points of the two-element member, where the accuracy of bending deformation is mathematically guaranteed for two-point integration. The rest of the shiftings are done according to the flow of the ASI technique.

In this study, the ASI-Gauss technique is implemented into a finite element code in order to develop a more precise and less-calculation-time-consuming seismic collapse simulator. The purpose of this study is to verify the validity of the ASI-Gauss technique in seismic collapse problems and to construct a highly efficient structural design tool for framed structures under three-dimensional excitation. Simple numerical tests are carried out to show the validity of the simulator, and an analysis involving member fracture and contact is performed on a large-scale framed structure to compare the effects of three-dimensional excitation against two-dimensional excitation.

2. NUMERICAL METHOD

General concept of the ASI-Gauss technique in comparison with the ASI technique is explained in this section. Moreover, algorithms considering member fracture and elemental contact, and incremental equation of motion for excitation at fixed points, are described.
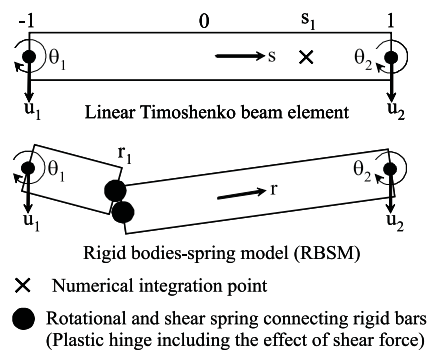

Figure 1 Linear Timoshenko beam element and its physical equivalent

2.1. ASI-Gauss Technique

Figure 1 shows a linear Timoshenko beam element and its physical equivalence to the rigid bodies-spring model (RBSM). As shown in the figure, the relationship between the locations of the numerical integration point and the stress evaluation point where a plastic hinge is actually formed is expressed as [12]

$$r = -s \tag{2.1}$$

In the above equation, *s* is the location of the numerical integration point and *r* the location where stresses and strains are actually evaluated. We refer to *r* as the stress evaluation point later in this paper. *s* and *r* are nondimensional quantities, which take values between -1 and 1.

In both the ASI and ASI-Gauss techniques, the numerical integration point is shifted adaptively when a fully plastic section is formed within an element to form a plastic hinge exactly at that section. When the plastic hinge is determined to be unloaded, the corresponding numerical integration point is shifted back to its normal position. Here, the normal position means the location where the numerical integration point is placed when the element acts elastically. By doing so, the plastic behavior of the element is simulated appropriately, and the converged solution is achieved with only a small number of elements per member. However, in the ASI technique, the numerical integration point is placed at the midpoint of the linear Timoshenko beam element, which is considered to be optimal for one-point integration, when the entire region of the element behaves elastically. When the number of elements per member is very small, solutions in the elastic range are not accurate since one-point integration is used to evaluate the low-order displacement function of the beam element.

The main difference between the ASI and ASI-Gauss techniques lies in the normal position of the numerical integration point. In the ASI-Gauss technique, two consecutive elements forming a member are considered as a subset, and the numerical integration points of an elastically deformed member are placed such that the stress evaluation points coincide with the Gaussian integration points of the member. This means that stresses and strains are evaluated at the Gaussian integration points of elastically deformed members. Gaussian integration points are optimal for two-point integration and the accuracy of bending deformation is mathematically guaranteed [13]. In this way, the ASI-Gauss technique takes advantage of two-point integration while using one-point integration in actual calculations.
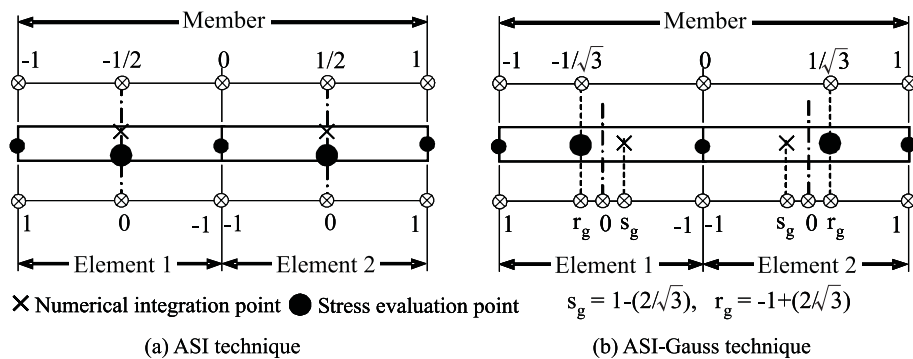

(a) ASI technique   (b) ASI-Gauss technique

Figure 2 Locations of numerical integration and stress evaluation points in elastic range

Figure 2 shows the locations of the numerical integrations points of elastically deformed elements in the ASI and ASI-Gauss techniques. The elemental stiffness matrix, generalized strain and resultant force increment vectors for the ASI technique are given by Eqn. 2.2 and those for the ASI-Gauss technique by Eqn. 2.3.

$$[K] = L[B(0)]^T[D(0)][B(0)] \tag{2.2a}$$

$$\{\Delta\varepsilon(0)\} = [B(0)]\{\Delta u\} \tag{2.2b}$$

$$\{\Delta\sigma(0)\} = [D(0)]\{\Delta\varepsilon(0)\} \tag{2.2c}$$

$$[K] = L[B(s_g)]^T[D(r_g)][B(s_g)] \tag{2.3a}$$

$$\{\Delta\varepsilon(r_g)\} = [B(s_g)]\{\Delta u\} \tag{2.3b}$$

$$\{\Delta\sigma(r_g)\} = [D(r_g)]\{\Delta\varepsilon(r_g)\} \tag{2.3c}$$

$$s_g = 1 - \frac{2}{\sqrt{3}}, \quad r_g = -1 + \frac{2}{\sqrt{3}} \tag{2.3d}$$

Here, $\{\Delta\varepsilon\}, \{\Delta\sigma\}$ and $\{\Delta u\}$ are the generalized strain increment vector, generalized stress (resultant force) increment vector and nodal displacement increment vector, respectively. $[B]$ is the generalized strain-nodal displacement matrix, $[D]$ the stress-strain matrix and L is the length of the element.
The plastic potential used in this study is expressed by

$$f = \left(\frac{M_x}{M_{x0}}\right)^2 + \left(\frac{M_y}{M_{y0}}\right)^2 + \left(\frac{N}{N_0}\right)^2 - 1 = f_y - 1 = 0 \tag{2.4}$$

Here, f_y is the yield function, and M_x, M_y and N are the bending moments around the x- and y- axes and axial force, respectively. Those with the subscript 0 are values that result in a fully plastic section in an element when they act on a cross section independently. The effect of torsion and shear force is neglected in the yield function.

2.2. Member Fracture and Contact Algorithm

(a) Elastic stage   (b) Plastic stage   (c) Member fracture
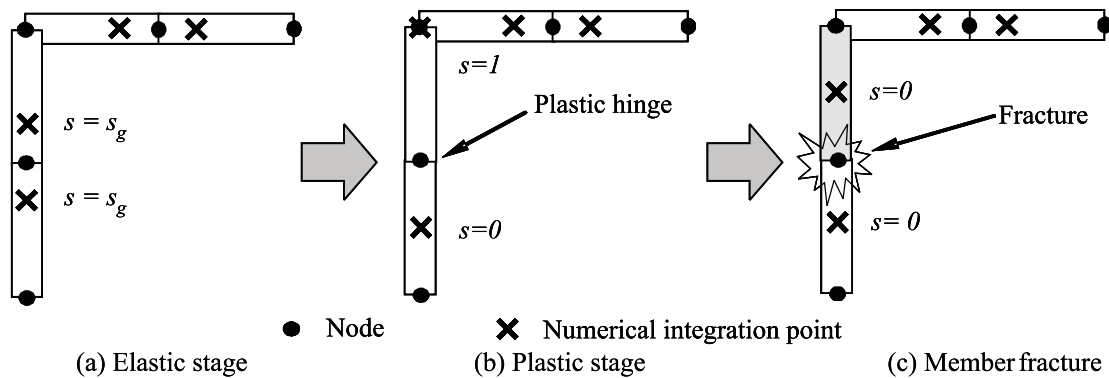
● Node   ✖ Numerical integration point

Figure 3 Locations of numerical integration points in each stage

A plastic hinge is likely to occur before it develops to a member fracture, and the plastic hinge is expressed by shifting the numerical integration point to the opposite end of the fully-plastic section. Accordingly, the numerical integration point of the adjacent element forming the same member is shifted back to its midpoint where it is appropriate for one-point integration. Figure 3 shows the locations of numerical integration points for each stage in the ASI-Gauss technique.
Member fracture is determined, in this study, by means of curvatures, shear strains and axial tensile strain occurred in the elements as shown in the following equation.

$$\left|\frac{\kappa_x}{\kappa_{x0}}\right| - 1 \geq 0 \ \ \text{or} \ \ \left|\frac{\kappa_y}{\kappa_{y0}}\right| - 1 \geq 0 \ \ \text{or} \ \ \left|\frac{\gamma_{xz}}{\gamma_{xz0}}\right| - 1 \geq 0 \ \ \text{or} \ \ \left|\frac{\gamma_{yz}}{\gamma_{yz0}}\right| - 1 \geq 0 \ \ \text{or} \ \ \frac{\epsilon_z}{\epsilon_{z0}} - 1 \geq 0 \tag{2.5}$$

where κ_x, κ_y, γ_{xz}, γ_{yz}, ε_z, κ_{x0}, κ_{y0}, γ_{xz0}, γ_{yz0} and ε_{z0} are the curvatures around the x- and y-axes, the shear strains for the x- and y-axes, the axial tensile strain and the critical values for these strains, respectively. We fixed the critical values using the information from actual experimental data [14]. Contact determination is done by examining the geometrical locations of the elements and once two elements are determined to be in contact, they are bound with a total of four gap elements between the nodes [10,11].

2.3. Incremental Equation of Motion

The dynamic equilibrium equation at time step $t=t$ can be formulated as

$$[M]\{\ddot{u}\}_t = \{E\}_t - \{F\}_t \tag{2.6}$$

where $[M]$, $\{\ddot{u}\}_t$, $\{E\}_t$ and $\{F\}_t$ are the mass matrix, acceleration vector, nodal external force vector and internal force vector at time step $t=t$, respectively.

The following equation is substituted into Eqn. 2.6 at $t=t+1$ in the implicit code:

$$\{F\}_{t+1} = \{F\}_t + [K]\{\Delta u\} \tag{2.7}$$

Then the following incremental stiffness equation is evaluated:

$$[M]\{\ddot{u}\}_{t+1} + [K]\{\Delta u\} = \{E\}_{t+1} - \{F\}_t \tag{2.8}$$

where $[K]$ is a stiffness matrix at time step $t=t$. By neglecting residual forces, an implicit code is obtained by evaluating the following incremental equation of motion:

$$[M]\{\Delta \ddot{u}\} + [K]\{\Delta u\} = 0 \tag{2.9}$$

Consequently, the incremental equation of motion for a structure under excitation at fixed points, which is used in this paper, yields to:

$$[M_1]\{\Delta \ddot{u}\} + [M_2]\{\Delta \ddot{u}_b\} + [K_1]\{\Delta u\} + [K_2]\{\Delta u_b\} = 0 \tag{2.10}$$

The subscript '1' indicates the coupled terms between free nodal points, '2' indicates the coupled terms between free nodal and fixed nodal points, and 'b' indicates the components at fixed nodal points. Vectors $\{\Delta \ddot{u}\}$ and $\{\Delta u\}$ are the nodal acceleration increment and the nodal displacement increment, respectively.

Under the assumption that the displacements at free nodal points are estimated by adding quasi-static displacement increments $\{\Delta u_s\}$ and dynamic displacement increments $\{\Delta u_d\}$, the displacements at free nodal points are given as

$$\{\Delta u\} = \{\Delta u_s\} + \{\Delta u_d\} \tag{2.11}$$

$\{\Delta u_s\}$ is evaluated, by neglecting inertia force, as follows:

$$\{\Delta u_s\} = -[K_1]^{-1}[K_2]\{\Delta u_b\} \tag{2.12}$$

Substituting Eqn. 2.11 and Eqn. 2.12 into Eqn. 2.10, the following equation is obtained:

$$[M_1]\{\Delta \ddot{u}_d\} + [K_1]\{\Delta u_d\} = ([M_1][K_1]^{-1}[K_2] - [M_2])\{\Delta \ddot{u}_b\} \tag{2.13}$$

In this scheme, equivalent forces are calculated by substituting nodal acceleration increments at fixed points into the right side of the above equation. Damping matrices are not considered in this study.

This derivation process above is made under the condition of neglecting residual forces, which consequently neglects the influence of gravity in collapse phenomena. The numerical analyses in previous work [10] are all performed by including the residual forces in vertical directions to consider the gravitational effects, under the restriction that the seismic wave in vertical direction can not be used as an input simultaneously. To enable the consideration of vertical seismic wave and gravitational effects at the same time, the calculations of the equations of motion under a seismic wave and dead load are separated in this paper; the equation of motion of a structure subjected under dead load is calculated according to Eqn. 2.8 and the obtained residual forces are added to the external forces calculated by Eqn. 2.13. The residual forces occurred by dead load are only considered while those occurred by seismic excitation are neglected. By using this approach, a simultaneous consideration of vertical seismic wave and gravitational effects became possible. All calculations in this paper are performed using this new approach.

3. NUMERICAL ESTIMATIONS

To verify the numerical code using the ASI-Gauss technique described in the previous section, elasto-plastic response analyses of a simple space frame under seismic excitation are performed. In the analyses, we use the following three schemes to verify the accuracy of the ASI-Gauss technique: (a) a conventional finite element scheme in which the numerical integration point of each element is fixed at its midpoint; (b) the ASI technique; and (c) the ASI-Gauss technique. An EW component of JMA Kobe seismic wave is multiplied by 1.5 for the amplitude and subjected at the fixed points according to Eqn. 2.10 to Eqn. 2.13. An implicit solution scheme using Newmark's β method (β=4/9 and δ=5/6 is used to consider numerical damping), updated Lagrangian formulation, and a consistent mass matrix are adopted in the analyses.

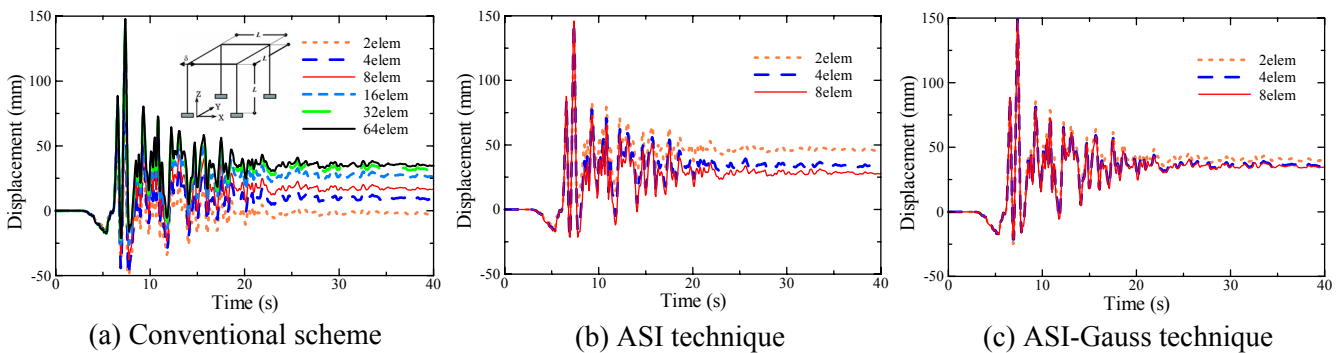| (a) Conventional scheme	(b) ASI technique	(c) ASI-Gauss technique

Figure 4 Comparison of the numerical accuracies between three schemes

Figure 4 shows the results of the analyses. Since plastic hinges are expressed only at the midpoints of the elements, the conventional scheme shows a very slow convergence and it finally converges when the 64-element modeling is used. The ASI technique gives comparatively better results than the conventional scheme. However, the two-element modeling yet does not give converged solution, since the elements lack with accuracy in the elastic range. On the other hand, the ASI-Gauss technique shows a very fast convergence and a converged solution is obtained with the minimum subdivision, since the stress evaluation points in the elements are adaptively controlled in both elastic and plastic ranges. The three-dimensional excitation gave the same tended results.
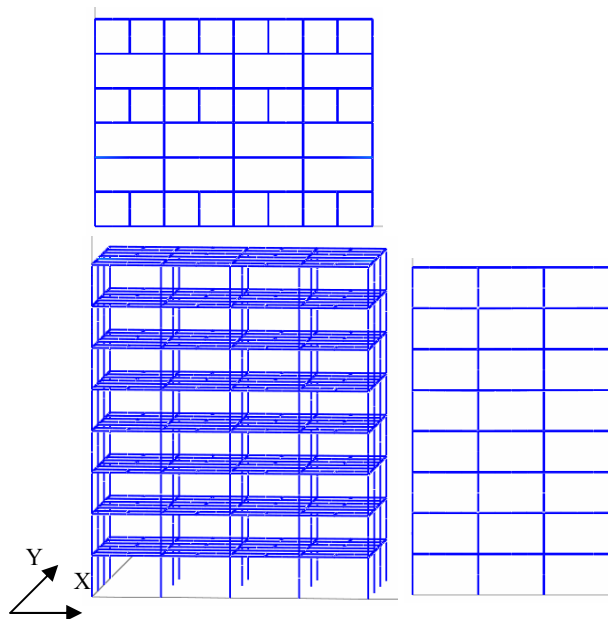
Figure 5 Eight-story frame model [15]

Table 1 Member list of typical columns

Floor	
8	$\square-450 \times 450 \times 12$
7	
6	$\square-500 \times 500 \times 12$
5	
4	$\square-500 \times 500 \times 16$
3	
2	
1	$\square-550 \times 550 \times 16$
Material	BCP325

Table 2 Member list of typical beams

Floor	
R	$H-400 \times 200 \times 9 \times 16$
8	
7	$H-600 \times 200 \times 12 \times 19$
6	
5	
4	
3	$H-600 \times 250 \times 12 \times 19$
2	
Material	SN490B

4. SEISMIC COLLAPSE ANALYSIS OF A LARGE-SCALE FRAMED STRUCTURE
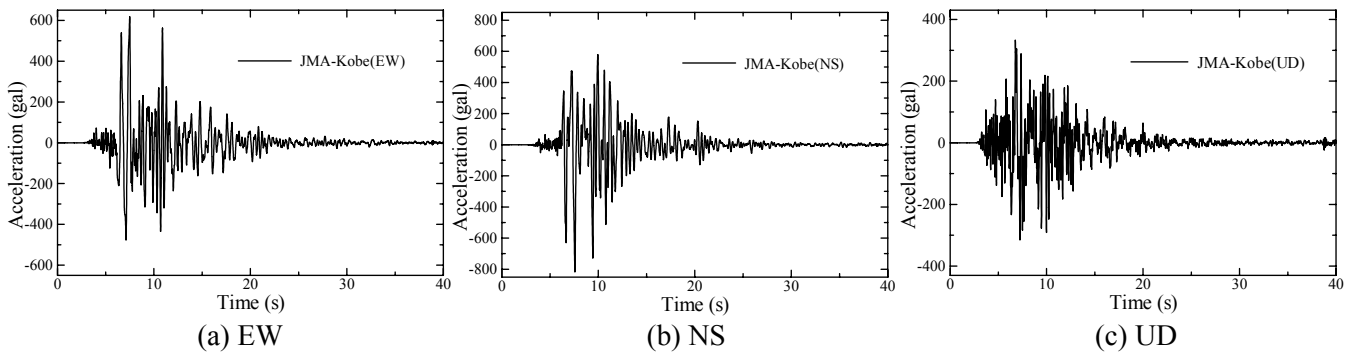

(a) EW　　　　　　　　　　(b) NS　　　　　　　　　　(c) UD

Figure 6 JMA-Kobe seismic wave (EW, NS, UD components)

A seismic collapse analysis is carried out on a 30 m high, 8-story steel framed structure [15], and three-dimensional excitation effect in collapse phenomena is verified by comparing with two-dimensional excitation result. The general view of the model is shown in Fig. 5 and the member lists of the typical columns and beams are shown in Table 1 and 2. The sectional sizes of the columns at the 3rd floor are deliberately set to 70% of the values in the table, in order to induce member fracture. EW, NS and UD components of JMA Kobe seismic wave shown in Fig. 6 are multiplied by 2.0 for the amplitude, and are subjected orthographically (EW to X-direction, NS to Y-direction and UD to Z-direction) at the fixed points on the ground floor. Dead load for each floor is assumed as 8.0 kN/m^2. The time increment is set to 5 ms and the calculation is done for a total of 8000 steps. The calculation takes approximately 80 CPU minutes with a personal computer (Core2 DUO E6300, 1.86 GHz CPU × 2, 3 GB RAM).
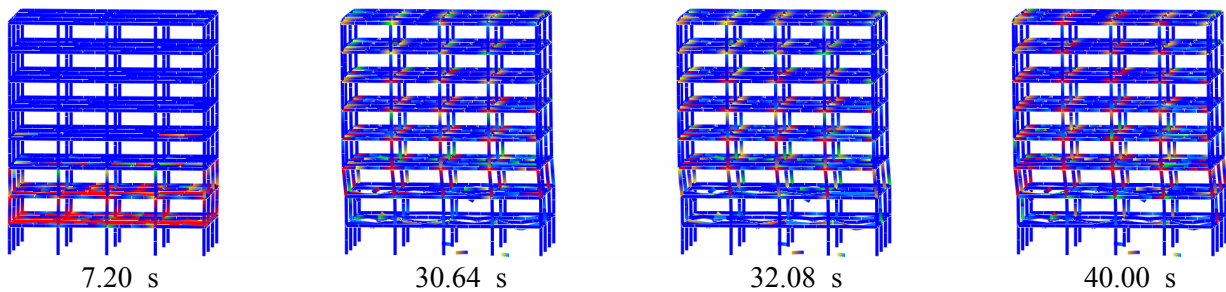

7.20 s　　　　　　　30.64 s　　　　　　　32.08 s　　　　　　　40.00 s

Figure 7(a) Seismic collapse analysis under two-dimensional seismic wave

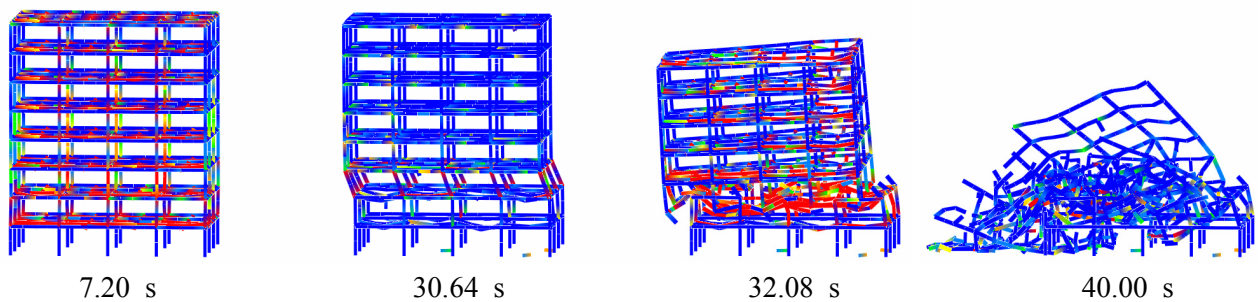7.20 s　　　　　　　30.64 s　　　　　　　32.08 s　　　　　　　40.00 s

Figure 7(b) Seismic collapse analysis under three-dimensional seismic wave

Figures 7(a) and 7(b) show the result under two-dimensional (EW and NS) excitation and the result under three-dimensional excitation, respectively. Fractured elements are excluded from the figures. Many plastic sections appear and some beams fracture in the two-dimensional excitation case, however, the structure withstands the excitation and does not collapse. But in the three-dimensional excitation case, the gravitational effect and the small vibration after the peak pulse gradually enlarges the deformation on the 3rd floor, where the

sectional sizes of the columns are deliberately lessened, and finally, failure initiates at approximately 30 s. This means that the UD component of the seismic wave cannot be neglected if the amplitude of the seismic wave particularly in vertical direction is considerably large.

5. CONCLUSIONS

In this paper, a nonlinear finite element seismic collapse simulator using the ASI-Gauss technique was developed, in order to analyze seismic collapse problems including structural discontinuities. The proposed simulator was improved by separating the calculation of the equations of motion for vertical seismic wave and dead load, to enable the consideration of both effects at the same time. The simulator gives accurate and practically realistic results in a short calculation time, which may be valid when used in a numerical estimation of the seismic design of large-scale framed structures. However, the damping matrices, as well as more detailed member properties such as local buckling, should also be considered in the future studies to improve the practicability.

REFERENCES

[1] Cundall, P.A. (1971). A Computer Model for simulating Progressive, Large-scale Movement in Blocky Rock System, *Proceedings of the International Symposium on Rock Mechanics* **II-8**, 129-136.
[2] Shi, G.H. and Goodman, R.E. (1984). Discontinuous Deformation Analysis, *Proceedings of 25th U.S. Symposium on Rock Mechanics*, 269-277.
[3] Meguro, K. and Hakuno, M. (1991). Simulation of Collapse Process of Structures due to Earthquake, *Proceedings of Symposium on Computational Methods in Structural Engineering and Related Fields*, **15**, 325-330, in Japanese.
[4] Ma, M.Y., Barbeau, P. and Penumadu, D. (1995). Evaluation of Active Thrust on Retaining Walls using DDA, *Journal of Computing in Civil Engineering*, **1**, 820-827.
[5] Yarimer, E. (1989). Demolition by Controlled Explosion as a Dynamical Process, *Structures under Shock and Impact*, 411-416.
[6] Tosaka, N., Kasai Y. and Honma, T. (1988). Computer Simulation for Felling Patterns of Building, *Demolition Methods and Practice*, 395-403.
[7] Toi, Y. and Isobe, D. (1993). Adaptively Shifted Integration Technique for Finite Element Collapse Analysis of Framed Structures, *International Journal for Numerical Methods in Engineering*, **36**, 2323-2339.
[8] Toi, Y. and Isobe, D. (1996). Finite Element Analysis of Quasi-static and Dynamic Collapse Behaviors of Framed Structures by the Adaptively Shifted Integration Technique, *Computers and Structures*, **58:5**, 947-955.
[9] Isobe, D. and Toi, Y. (2000). Analysis of Structurally Discontinuous Reinforced Concrete Building Frames using the ASI Technique, *Computers and Structures*, **76:4**, 471-481.
[10] Isobe, D. and Tsuda, M. (2003). Seismic Collapse Analysis of Reinforced Concrete Framed Structures Using the Finite Element Method, *Earthquake Engineering and Structural Dynamics*, **32:13**, 2027-2046.
[11] Isobe, D. and Lynn, K.M. (2004). A Finite Element Code for Structural Collapse Analyses of Framed Structures under Impact Loads, *Proceedings of the 4th European Congress on Computational Methods in Applied Sciences and Engineering (ECCOMAS 2004)*, Jyvaskyla, Finland.
[12] Toi, Y. (1991). Shifted Integration Technique in One-Dimensional Plastic Collapse Analysis using Linear and Cubic Finite Elements, *International Journal for Numerical Methods in Engineering*, **31**, 1537-1552.
[13] Press, W.H., Teukolsky, S.A., Vetterling, W.T. and Flannery, B.P. (1992). Numerical Recipes in FORTRAN: The Art of Scientific Computing, 2nd Edition, Cambridge University Press.
[14] Hirashima, T., Hamada, N., Ozaki, F., Ave, T. and Uesugi, H. (2007). Experimental Study on Shear Deformation Behavior of High Strength Bolts at Elevated Temperature, *Journal of Structural and Construction Engineering*, **621**, 175-180, in Japanese.
[15] Kaitani, J. *et al*. (2006). Design Example and Earthquake Response of the Frames with Knee Damper Part 2: Design Examples of 8-Story Office Building, *Summaries of Technical Papers of Annual Meeting Architectural Institute of Japan 2006*, **C-1**, 753-754, in Japanese.